01 Mar 2000

A High Energy X-Ray and Neutron Scattering Study of Iron Phosphate Glasses Containing Uranium

Mevlüt Karabulut

G. K. Marasinghe

C. S. Ray
Missouri University of Science and Technology, csray@mst.edu

Y. S. Badyal

et. al. For a complete list of authors, see https://scholarsmine.mst.edu/matsci_eng_facwork/1457

A high energy x-ray and neutron scattering study of iron phosphate glasses containing uranium

M. Karabulut,[a] G. K. Marasinghe, C. S. Ray, G. D. Waddill, and D. E. Day
Department of Physics, Department of Ceramic Engineering, and the Graduate Center for Materials Research, University of Missouri-Rolla, Rolla, Missouri 65401-1170

Y. S. Badyal, M.-L. Saboungi, S. Shastri, and D. Haeffner
Argonne National Laboratory, Argonne, Illinois 60439

(Received 2 July 1999; accepted for publication 21 November 1999)

The atomic structure of iron phosphate glasses containing uranium has been studied by complementary neutron and x-ray scattering techniques. By combining x-ray and neutron structure factors, detailed information about different pair interactions has been obtained. Most of the basic structural features such as coordination numbers and O–O and P–O distances in uranium containing glasses are the same as those in the base glass of batch composition $40Fe_2O_3$–$60P_2O_5$ (mol %). However, the Fe–O distances change slightly with the addition of uranium. The observed structural parameters support a structural model in which the waste elements occupy voids in the Fe–O–P network, hence, not altering the basic structure of the parent iron phosphate glass. © *2000 American Institute of Physics.* [S0021-8979(00)02605-0]

I. INTRODUCTION

Interest in phosphate based host matrices for the vitrification of nuclear wastes started in the 1960s with sodium phosphate glasses.[1] However, their low chemical durability and high corrosiveness resulted in the exclusion of this family of glasses from the pool of host matrices intended to vitrify nuclear wastes. Lead-iron phosphate glasses were one of the promising vitreous phosphate materials considered as a host matrix for high level nuclear wastes (HLW).[1–4] The chemical durability of these glasses, many orders of magnitude better than that of common phosphate glasses, is comparable to that of borosilicate glasses, the only host matrix currently approved by the U.S. Department of Energy. However, the low waste loading, the low corrosion resistance of their crystallized counterparts, and the limited experience in melting lead-iron phosphate glasses led to their exclusion from use in the current vitrification program.[5]

In contrast to lead-iron phosphate glasses, binary iron phosphate glasses of approximate composition xFe_2O_3–$(100-x)P_2O_5$ ($x>30$ mol %) possess all the properties required of a suitable host matrix. For example, iron phosphate glasses can be melted at temperatures as low as 1100 °C and in excess of 40 wt % of certain types of HLWs poorly soluble in borosilicates can be added without adversely affecting their chemical durability.[6,7] The chemical durability of iron phosphate nuclear waste forms and their crystalline counterparts is comparable to, or better than, that of many common borosilicate based wasteforms.[7]

The atomic structure of binary iron phosphate glasses has been investigated recently using Mössbauer, x-ray photoelectron (XPS), x-ray absorption fine structure and Raman spectroscopic techniques.[6–10] Both Fe^{2+} and Fe^{3+} ions are present in these glasses with a $Fe^{2+}/(Fe^{2+}+Fe^{3+})$ ratio of 0.15–0.35. Both species of iron ions are coordinated with 5–6 near neighbor oxygens.[6,8,9] The Fe–O polyhedra are interconnected via $(P_2O_7)^{4-}$ units which dominate the P–O network.[8] In contrast to the atomic structure of common phosphate glasses where the majority of oxygen ions are bonded via easily hydrated –P–O–P– bonds,[11] the majority of the oxygens in binary iron phosphate glasses appear to be forming hydration resistant –Fe–O–P– bonds.[6–10] The purpose of the present work is to investigate the detailed structure of iron phosphate glasses with and without uranium in order to determine changes induced by the waste elements in the structure of the host matrix.

One of the difficulties encountered when studying the structure of a *n*-component disordered system is that a single diffraction measurement gives a weighted, $S(Q)$, average of $n(n+1)/2$ separate partial structure factors, $S_{ij}(Q)$.[12–14] $S(Q)$ is given by

$$S(Q)=\sum_{ij} W_{ij}S_{ij}(Q), \tag{1}$$

where the W_{ij} are the weighting factors which are generally constant in the case of neutrons and depend on Q in the case of x-rays. Under favorable conditions, both approaches can be used in a complementary fashion to resolve the atomic structure to a greater extent. Since the weighting factors may vary among elements in a quite different way for neutrons and x-rays, combining these two techniques makes it possible to identify specific features in the partial pair distribution due to the differences in the weighting factors.[12,15,16]

II. EXPERIMENTAL DETAILS

The glasses listed in Table I were prepared by melting homogeneous mixtures of reagent grade chemicals in dense alumina crucibles at 1200 °C in air for approximately 2 h.

[a]Author to whom correspondence should be addressed; electronic mail: mevlutk@umr.edu

TABLE I. Batch compositions of the glasses studied. The compositions of selected samples were checked by EDAX and the results are given in parentheses. The bulk density of each glass and the calculated number density for the samples used in neutron diffraction experiments are also given in the last two columns.

Sample	Batch composition (mol %)				Fe/P ratio	ρ (g/cm^3) (±5%)	ρ_0 (atoms/Å^3)
	Fe_2O_3	Fe_3O_4	P_2O_5	UO_2			
A	40	0	60	0	0.66	3.10	0.0277
B	36	0	54	10	0.66	3.32	0.0263
C	32.4	0	48.6	19	0.66	3.39	0.0257
D	0	27.7	62.3	10	0.66	3.29	⋯
E	0	26.2	58.8	15	0.66	3.32	⋯
F	35 {36.3}	0	60 {59}	5{4.63}	0.58	3.12	⋯
G	30 {33.8}	0	60 {57}	10{9.8}	0.50	3.24	⋯
H	25	0	60	15	0.42	3.33	⋯

Each melt was poured into 1 cm×1 cm×5 cm steel molds, annealed at ~475 °C in air for ~3 h and slowly cooled to room temperature. Powders of annealed glasses were checked for crystalline phases by x-ray diffraction. The final compositions of selected glasses were checked by inductively coupled plasma spectroscopy and energy dispersive analysis of x-rays (EDAX) and showed good agreement with the batch composition.[17] Additional experiments were conducted to check the weight loss during melting which showed negligible weight loss (<2%). The density of each glass was measured by the Archimedes' method using water as the suspending medium. Neutron scattering data were collected from ~75 μm powders loaded into thin-walled vanadium containers. For the x-ray experiments, the glasses were shaped as plates with the side exposed to the x-ray beam polished to an approximate roughness of 50 μm.

The neutron scattering experiments were conducted using GLAD (glass, liquid, and amorphous materials diffractometer) at the Intense Pulsed Neutron Source (IPNS), Argonne National Laboratory (ANL).[18] The room temperature time-of-flight diffraction data were collected in groups of detectors fixed at scattering angles ranging from 8° to 125°, with a wavelength range of 0.15–3 Å. Measurements were conducted on the glasses, empty container, a vanadium standard for normalization purposes, and the instrument background. After subtracting the instrument background and empty container, diffraction from sample was corrected for absorption, multiple scattering, and inelasticity effects using standard procedures.[12–14,19] The paramagnetic scattering was subtracted from the data using procedures described in Ref. 20. The neutron weighted average structure factor $S^N(Q)$ was obtained from the total measured differential cross section

$$\frac{d\sigma}{d\Omega} = \langle \overline{b} \rangle^2 [S^N(Q) - 1] + \langle \overline{b^2} \rangle, \tag{2a}$$

where $\langle \overline{b} \rangle$ and $\langle \overline{b^2} \rangle$ are the mean and mean square neutron scattering length averaged over all atoms in the system. The wave vector Q is defined by the scattering angle 2θ and the neutron wavelength, λ, $Q = 4\pi \sin\theta/\lambda$.

The x-ray scattering measurements were carried out on the 1-BM bending magnet beamline at the Advanced Photon Source (APS) at ANL using a horizontally focusing, single bounce Si(111) monochromator with an energy of 61.332 keV ($\lambda = 0.2022$ Å). The experiments were conducted in flat-plate symmetrical transmission geometry with a solid-state Ge detector scanning in the vertical plane to minimize polarization corrections. The data were corrected for the detector dead time, attenuation, air scattering, multiple scattering, and Compton scattering. In this case, the x-ray weighted average structure factor $S^X(Q)$ was obtained form the measured differential cross section.

$$\frac{d\sigma}{d\Omega} = \langle f(Q) \rangle^2 [S^x(Q) - 1] + \langle f(Q)^2 \rangle, \tag{2b}$$

where $\langle f(Q) \rangle$ and $\langle f(Q)^2 \rangle$ are the mean and mean square x-ray scattering factors.

The real space differential correlation function is obtained from the $S(Q)$s for both neutron and x-ray data by Fourier transform

$$D(r) = \frac{2}{\pi} \int_{Q_{\min}}^{Q_{\max}} Q[S(Q) - 1] \sin(Qr) dQ. \tag{3a}$$

The total real space correlation function, $T(r) = \Sigma W_{ij} T_{ij}(r)$, then can be calculated from

$$T(r) = D(r) + 4\pi\rho_0 r, \tag{3b}$$

where ρ_0 is the total number density. The partial coordination numbers can be estimated from $T(r)$, using, for example, Gaussian fits of $T(r)$ and the weighting factors W_{ij}.

Room temperature Mössbauer experiments were conducted on a spectrometer that utilized a 50 mCi ^{57}Co source embedded in a rhodium matrix. The spectrum was calibrated at room temperature with metallic α-iron foil whose linewidth was 0.27 mm/s. Each Mössbauer spectrum was fitted with a minimum number of broadened paramagnetic Lorentzian doublets, usually eight, to match the absorption envelope with a missfit of less than 0.3%. It is important to note that these doublets are not assigned to specific iron sites. The experimental and fitting details about Mössbauer measurements are given elsewhere.[6]

III. RESULTS

The density and premelt composition of the glasses studied are summarized in Table I. Compositions of selected

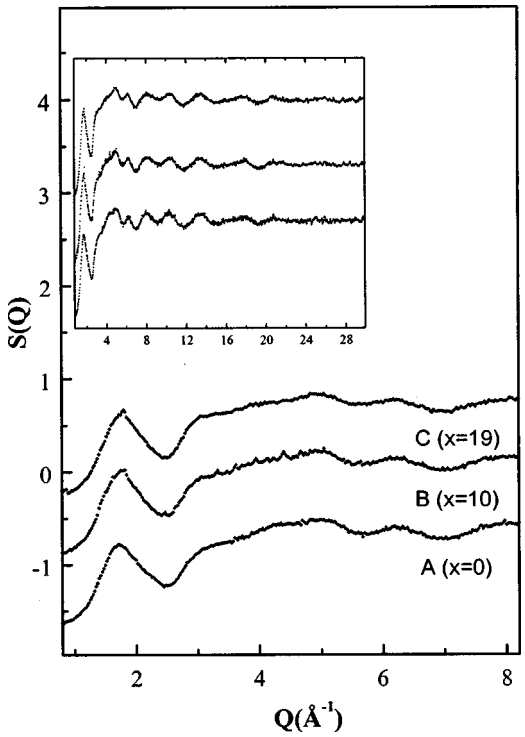

FIG. 1. The average neutron structure factors for the base glass and two uranium containing iron phosphate glasses $[(1-x)(40Fe_2O_3-60P_2O_5)-xUO_2,\ x=0,10,19,$ mol %]. The inset shows the full Q range without magnetic correction.

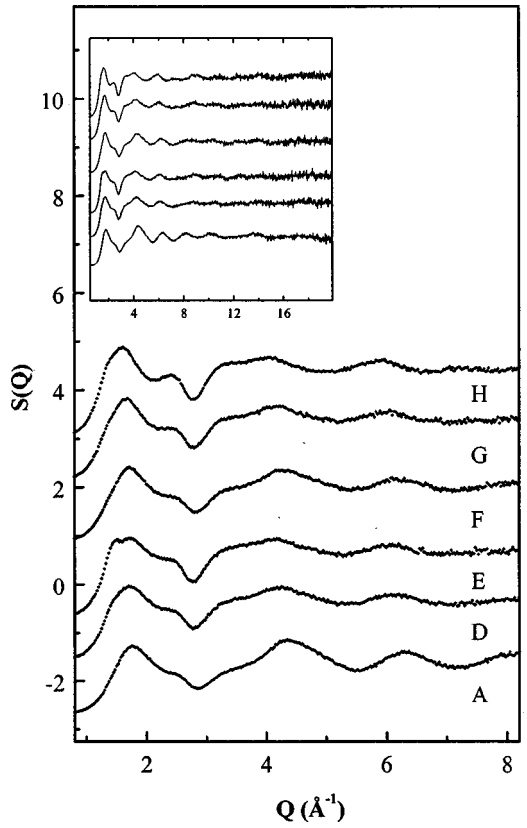

FIG. 2. The average x-ray structure factors for the base glass ($40Fe_2O_3-60P_2O_5$, mol %) and uranium containing iron phosphate glasses. The inset shows the full Q range. Refer to Table I for the compositions of the uranium containing glasses.

glasses as checked by EDAX are also given in Table I. Neutron measurements were made for glasses A, B, and C up to 30 Å^{-1} while x-ray measurements were made for the glasses A, D, E, F, G, and H up to 20 Å^{-1}. It must be noted that glasses B and D have very similar compositions, Fe/P $=0.66$ and 10 mol % UO_2, the only difference being the source of iron in the starting batch, Fe_2O_3 for glass B and Fe_3O_4 for glass D. Figures 1 and 2 show the neutron and x-ray average structure factors, $S^N(Q)$ and $S^X(Q)$, for the base glass (glass A) and uranium containing glasses, plotted up to 8 Å^{-1} to emphasize the structural features which appear at low Q. Full Q ranges are given as insets in Figs. 1 and 2. For the uranium containing glasses the average structure factors $S^N(Q)$ and $S^X(Q)$ are a weighted combination of $n(n+1)/2=10$ partial structure factors. The weighting factors, W_{ij}, for x-ray and neutron structure factors for selected glasses are given in Table II. Because of the difference in the neutron and x-ray scattering lengths, some of the partial structure factors contribute more to the average x-ray structure factor $S^X(Q)$ than to the average neutron structure factor $S^N(Q)$ (e.g., S_{U-O}, S_{U-P}, S_{Fe-P}) and vice-versa (e.g. S_{O-O}). In the present study, the difference between the neutron and x-ray average structure factors will be exploited to extract detailed information on local environment of specific atom pairs.

$S^N(Q)$ and $S^X(Q)$ for the base glass ($40Fe_2O_3$–$60P_2O_5$, mol %, sample A) shown in Figs. 1 and 2 contain two peaks, one at $Q\sim1.7$ Å^{-1} and the other at $Q\sim2.3$ Å^{-1}. The second peak is better resolved in $S^X(Q)$ than in $S^N(Q)$. The peak positions correspond to correlation lengths $(2\pi/Q)$ of 3.69 and 2.73 Å, respectively. The intensity of the peaks is stronger in $S^X(Q)$ than in $S^N(Q)$. While the addition of uranium does not affect the first peak position in $S^N(Q)$, it shifts to lower $Q(\sim1.66$ Å$^{-1})$ in $S^X(Q)$. The intensity of the second peak in $S^X(Q)$ increases with the uranium content.

Total correlation functions, $T^N(r)$ and $T^X(r)$ given in Fig. 3 were derived using Eqs. (2) and (3) with a Q range of 0.7–30 Å^{-1} for the neutrons and 0.7–20 Å^{-1} for the x-rays. $T^N(r)$ of the base glass (sample A) features four prominent peaks, a well resolved peak, at 1.53 Å, an asymmetric peak at 1.94 Å, and two peaks at 2.52 and 3.3 Å. A fifth peak, weak and unresolved, is situated at 2.9 Å. These features are

TABLE II. Neutron and x-ray weighting factors for glasses A, B, and D.

	W_{ij}^n		W_{ij}^x	
S_{ij}	A	B	A	D
O–O	0.408	0.403	0.215	0.174
Fe–O	0.255	0.240	0.266	0.210
P–O	0.206	0.193	0.230	0.185
Fe–P	0.065	0.057	0.143	0.111
Fe–Fe	0.040	0.035	0.082	0.063
P–P	0.026	0.023	0.061	0.049
U–O	⋯	0.029	⋯	0.091
Fe–U	⋯	0.008	⋯	0.054
U–P	⋯	0.007	⋯	0.048
U–U	⋯	0.0005	⋯	0.012

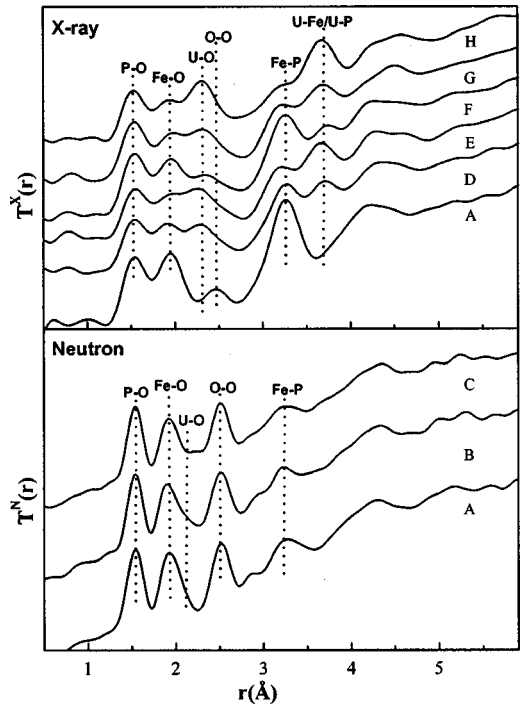

FIG. 3. The average real space neutron (bottom) and x-ray (top) correlation functions for the structure factors shown in Figs. 1 and 2. Q_{max} was 30 $Å^{-1}$ for neutrons and 20 $Å^{-1}$ for x rays.

seen to remain largely unchanged in position and width upon the addition of uranium (glasses B and C). However, an additional unresolved peak occurs at ~2.2 Å in $T^N(r)$ of these uranium containing glasses, while the intensity of the peak at 2.9 Å decreases as the UO_2 concentration increases (Fig. 3).

The positions of the peaks in $T^X(r)$ of the base glass, 1.52, 1.93, 2.45, and 3.3 Å, are quite similar to those of $T^N(r)$, but with different intensities reflecting differences in scattering lengths. The x-ray results emphasize scattering from the heavy atoms. Addition of uranium causes two additional peaks to appear at 2.26 and 3.7 Å, respectively, whose intensity increase with the uranium content. These peaks are also observed in neutron $T(r)$ but with very low intensities. The asymmetry noticed in the second peak of $T^N(r)$ is not present in $T^X(r)$.

If a peak in $T(r)$ of an amorphous material can be assigned to a distinct atomic pair by comparing to a crystalline material, the coordination number C_{ij} can be calculated from Gaussian fits of $T(r)$, as discussed elsewhere.[12–14,21] In the neutron case

$$C_{ij} = N\langle \overline{b} \rangle^2 / 2 c_i b_i b_j , \tag{4}$$

where N is the area $\int rT(r)dr$ for the peak considered and the c_i denote the concentration of the ith component.

In the present study, the crystal structure of $Fe_3(P_2O_7)_2$,[22] a mixed-valence pyrophosphate which shares features in short range order with the base glass, is used to assign peaks in $T(r)$ to distinct atom pairs. This phase crystallizes when the base glass is heat treated in air at 600 °C for 24 h.[6,17]

The crystalline structure of $Fe_3(P_2O_7)_2$ features P–O distances ranging from 1.48 to 1.59 Å, Fe^{2+}–O and Fe^{3+}–O distances ranging from 2.09 to 2.13 Å and 1.88 to 1.91 Å, respectively, O–O distances ranging from 2.5 to 2.9 Å, and Fe–P distances ranging from 3.2 to 3.5 Å. Based on these interatomic distances and weighting factors given in Table II, the four prominent peaks in $T^N(r)$ and $T^X(r)$ of the base glass, present also in uranium containing glasses, are assigned to P–O (1.53 Å), Fe–O (1.94 Å), O–O (2.52 Å), and Fe–P (3.3 Å) correlations. The intensity of the peak arising from the Fe–P correlation observed at 3.3 Å in both $T^N(r)$ and $T^X(r)$ is consistent with the x-ray and neutron weighting factors, the neutron weighting factor for Fe–P being about four times lower than the x-ray weighting factor. The existence of Fe–P peak in uranium containing glasses indicates that –Fe–O–P– type bonding, which is believed to be essential for the chemical durability of the base glass, is also maintained in uranium containing glasses. The intensity of Fe–P peak diminishes proportionally with the decreasing concentration of iron and phosphorus (Fig. 3).

As mentioned earlier, the uranium containing iron phosphate glasses have two additional peaks in both neutron and x-ray $T(r)$ (2.26 and 3.7 Å), with much better resolution in $T^X(r)$ than in $T^N(r)$. Based on known structures of some uranium compounds,[23] the peak observed at around 2.26 Å in $T^X(r)$ is assigned to U–O correlation, while the peak at ~3.7 Å cannot be uniquely identified as a single correlation. Most probably it is due to correlations involving U–P and/or U–Fe rather than U–U.

Based on these peak assignments, the coordination numbers C_{ij} were calculated using Eq. (4). In order to eliminate effects of different resolution between the neutron and x-ray $T(r)$, the same value of $Q_{max}=20\,Å^{-1}$ was used in Fourier transforms to obtain $T^X(r)$ and $T^N(r)$. The $T(r)$s were fit with deconvolved Gaussians and the values obtained are summarized in Tables III and IV.

More structural details can be obtained by first order differencing of the neutron and x-ray data taking advantage of the contrast in scattering lengths to eliminate at least one of the partial terms in the summation describing the average scattering [see Eq. (1)]. This must be done with the data obtained from glasses having similar compositions since the partial pair scattering factors are expected to change with composition. For the base glass, this procedure can be used to eliminate the O–O partial contribution. Figure 4 shows the difference total correlation function $\Delta T(r)$ obtained by the Fourier transform of $\Delta S(Q)$ which makes it possible to distinguish the Fe–O and Fe–P peaks much less ambiguously. The spectrum was fit with deconvolved Gaussians which are also given in Fig. 4 as dotted lines. Clearly there are two partially resolved peaks under the second peak labeled as Fe–O_s (short) and Fe–O_l (long) at 1.92 and 2.29 Å (±0.02 Å), respectively.

The U–O, O–O, and Fe–O partial correlations in $T^N(r)$ and $T^X(r)$ of uranium containing glasses are not well resolved. Glasses B and D (10 mol% UO_2) have very similar atomic compositions. Thus, the $S^N(Q)$ of glass B and $S^X(Q)$ of glass D can be used to obtain approximate differences, as was done for the base glass earlier, to resolve these correlations more clearly. First, the O–O term was eliminated and the resulting difference correlation function, $\Delta T(r)$, and fits

TABLE III. Structural parameters obtained from $T^N(r)$.

Sample	A		B		C	
(ij)	C_{ij}	R_{ij}	C_{ij}	R_{ij}	C_{ij}	R_{ij}
P–O	3.8±0.2	1.53±0.01	3.6±0.2	1.53±0.01	3.4±0.2	1.53±0.01
Fe–O	4.7±0.3	1.94±0.02	4.4±0.3	1.92±0.02	3.9±0.3	1.92±0.02
U–O	···	···	4.2±0.4	2.17±0.02	4.0±0.4	2.19±0.02
O–O	5.0±0.5	2.52±0.02	5.0±0.5	2.52±0.02	3.9±0.5	2.51±0.02

are shown in Fig. 5. The P–O peak remains at nearly the same position as in the base glass with a coordination number of ~4.1 (±0.2) confirming that the local environment around phosphorus is not significantly disturbed. The Fe–O_s and Fe–O_l distances seen in the base glass cannot be separated due to the overlap of Fe–O and U–O peaks. However, an average coordination number of 5.28 (±0.3) was obtained by fitting a single broad Gaussian which indicates that the Fe–O environment in uranium containing glasses remains similar to that in base glass. Next, the Fe–O partial contribution, which due to the order of taking the difference gives rise to a negatively weighted O–O pair correlation, was eliminated, see Fig. 6. In addition to the P–O and U–O peaks clearly visible at the expected positions, there appears to be another peak observed in $\Delta T(r)$ at around 1.77 Å. Since the Fe–O peak has been eliminated, this may be a contribution from correlations other than Fe–O. The mean separation distance of 1.77 Å is a typical U–O distance (~1.8 Å) observed in uranyl (UO_3) compounds including UO_2^{2+}.[23] In the starting batch the uranium source is UO_2, hence, the valence state of uranium is 4+. This peak may be an indication that some of the U^{4+} ions may have been oxidized to U^{6+} during the melting. However, the UL_{III}-edge x-ray absorption near edge structure (XANES) studies on some uranium containing iron phosphate glasses do not show any change in the uranium oxidation state. Figure 7 compares the UL_{III}-edge XANES spectra of glasses F, G, and H (5, 10, 15 mol % UO_2) to well characterized U^{4+} and U^{6+} references (UO_2 and UO_2^{2+} given as dotted and dashed lines, respectively) which clearly indicates that the uranium ions are dominantly tetravalent.

IV. DISCUSSION

A. Base glass

The first peak observed at $Q=1.74\,\text{Å}^{-1}$ in $S^N(Q)$ and $S^X(Q)$ of the base glass is similar to the peaks observed in earlier studies of phosphate glasses.[15,24,25] The intensity of the first peak is stronger in $S^X(Q)$ than in $S^N(Q)$. Considering the weighting factors given in Table II, this may suggest that this peak is related to cation-cation interaction, the correlation length being $2\pi/Q=3.69$ Å which is characteristic of intermediate range order in oxide glasses. These intermediate range order parameters are associated with the effective periodicity of the real space electron density fluctuations or with the spacing of quasi-Bragg planes.[26,27]

The structural parameters in Table III and IV indicate that the P–O coordination is close to tetrahedral. The different P–O distances in bridging, –P–O–P–, and nonbridging, –P–O–Fe–, bonds observed in the neutron diffraction study[6] of crystalline counterpart of the base glass, $Fe_3(P_2O_7)_2$, could not be resolved for the glasses studied here. However, the approximate oxygen coordination around phosphorus is close to the value of four for regular $(PO_4)^{3-}$ tetrahedra which connects with other tetrahedral units to form $(P_2O_7)^{4-}$ units in crystalline $Fe_3(P_2O_7)_2$ structure. Similar results were obtained from Raman and XPS spectroscopic studies of the base glass and some uranium containing glasses. The structure of the base glass and waste containing glasses were found to be similar and dominated by $(P_2O_7)^{4-}$ dimer units as in crystalline $Fe_3(P_2O_7)_2$.[28,29]

The structural parameters obtained from the neutron and x-ray $T(r)$s show that the oxygen coordination around iron is close to five. From the difference spectrum (Fig. 4), two

TABLE IV. Structural parameters obtained from $T^X(r)$.

	A		D		E		F		G		H	
(ij)	C_{ij}	R_{ij}	C_{ij}	R_{ij}	C_{ij}	R_{ij}	C_{ij}	R_{ij}	C_{ij}	R_{ij}	C_{ij}	R_{ij}
P–O	3.6	1.52	3.6	1.52	3.7	1.52	3.9	1.53	3.8	1.52	3.9	1.52
	±0.02	±0.01	±0.2	±0.01	±0.2	±0.01	±0.2	±0.01	±0.2	±0.01	±0.2	±0.01
Fe–O	4.6	1.93	4.7	1.91	4.7	1.90	5.1	1.94	6.4	1.97	5.3	1.91
	±0.3	±0.02	±0.3	±0.02	±0.3	±0.02	±0.3	±0.02	±0.3	±0.02	±0.3	±0.02
U–O	···	···	7.1	2.26	6.6	2.24	7.3	2.28	4.8	2.30	7.0	2.26
			±0.7	±0.04	±0.7	±0.04	±0.7	±0.04	±0.7	±0.04	±0.7	±0.04
O–O	5.0	2.45	4.8	2.52	5.3	2.52	5.0	2.52	4.8	2.52	4.8	2.52
	±0.5	±0.05	±0.5	±0.04	±0.5	±0.04	±0.5	±0.04	±0.5	±0.04	±0.5	±0.04

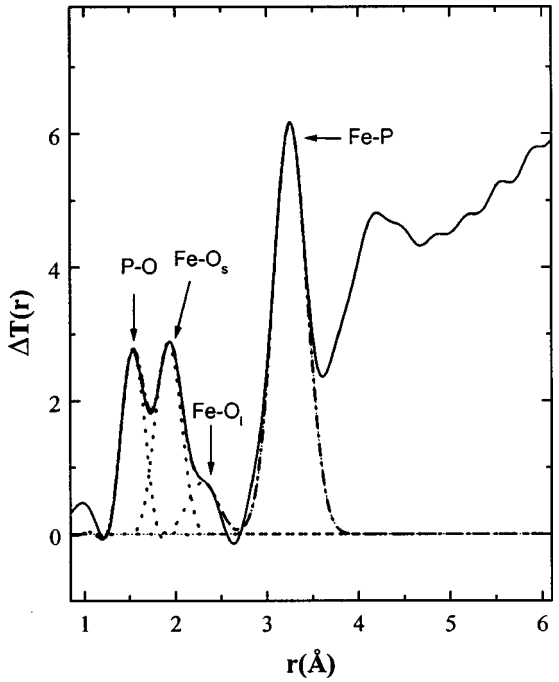

FIG. 4. The average real space neutron/x-ray difference spectrum and deconvolved Gaussian fits (dotted lines) for the base glass obtained by eliminating the O–O correlation using the weighting factors given in Table II. Clearly, two Fe–O distances are resolved at 1.92 and 2.29 Å.

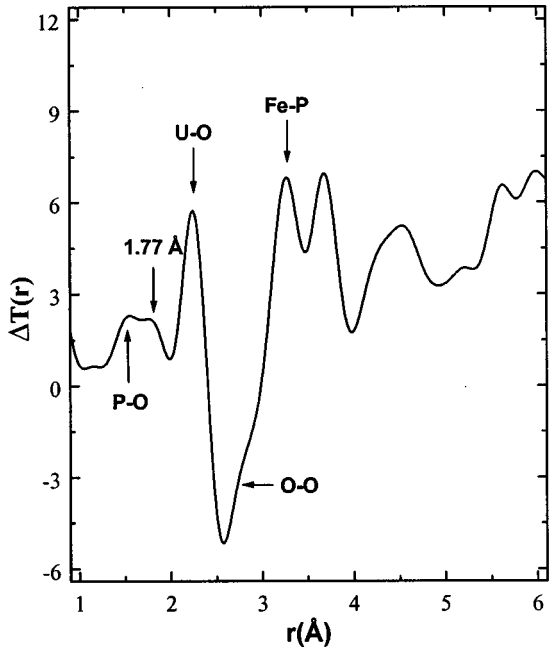

FIG. 6. The average real space neutron/x-ray difference spectrum obtained by eliminating the Fe–O correlation for the glasses B and D. Due to the order of taking the difference the O–O correlation is negative.

Fe–O peaks can be resolved with total coordination number of ~5.8 (±0.3), confirming Mössbauer results suggesting that iron ions are 5–6 coordinated with near-neighbor oxygens.[6,10] It is worth noting that the Fe–O coordination is six in $Fe_3(P_2O_7)_2$. The Fe–P local environment was not well resolved compared to the Fe–O and P–O environments. However, assuming no contributions from the other pair correlation terms, an upper limit of ~4.5(±0.6) for the phosphorus coordination around iron ions was obtained for the Fe–P peak in Fig. 4.

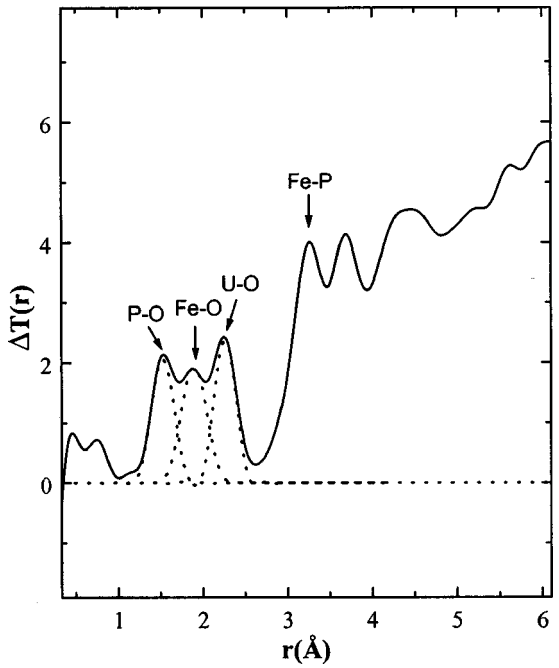

FIG. 5. The average real space neutron/x-ray difference spectrum and deconvolved Gaussian fits (dotted lines) obtained by eliminating the O–O correlation between the average structure factors of glass B ($36Fe_2O_3$–$54P_2O_5$–$10UO_2$,mol %) and glass D ($27.7Fe_3O_4$–$62.3P_2O_5$–$10UO_2$,mol %). Note that the Fe/P ratio in both glasses is 0.66.

The two Fe–O distances found in $\Delta T(r)$ (Fig. 4) agree with the recent Fe *K*-edge extended x-ray absorption fine structure (EXAFS) study of these iron phosphate glasses.[9] Table V compares the coordination numbers and mean pair separation distances for Fe–O and Fe–P measured in the present study to those obtained from EXAFS[9] and to those for the crystalline counterpart of the base glass.[6] Three Fe–O distances are resolved from the Fe *K*-edge EXAFS data while only two Fe–O distances are resolved from the difference spectrum of the neutron and x-ray data. The Fe–P distances are similar, however, the Fe–P coordination numbers obtained in the present study are lower than those obtained from the EXAFS study.

B. Uranium containing glasses

The structural parameters summarized in Tables III and IV indicate that the base glass and the uranium containing glasses have similar mean bond distances and coordination numbers. The approximate P–O, Fe–O, and U–O coordination numbers are four, five, and seven, respectively. The P–O and O–O mean bond distances do not change appreciably with the uranium content. However, both neutron and x-ray structural parameters indicate a small decrease (1.6%) in the Fe–O distance when uranium is substituted for both iron and phosphorus in the base glass, i.e., in glasses B, C, D, and E. A similar trend was observed in a recent EXAFS study of glasses D and E.[9] In contrast, the Fe–O distance

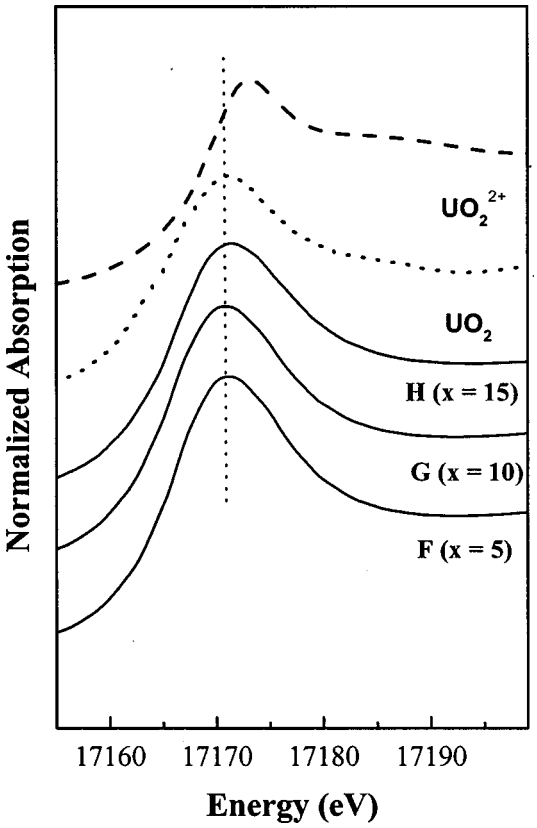

FIG. 7. Normalized UL_{III}-edge XANES spectra for three uranium containing iron phosphate glasses $[(40-x)Fe_2O_3-60P_2O_5-xUO_2, x=5,10,15,\text{mol}\,\%]$. The spectra are compared to that of two well-characterized reference compounds: UO_2 as U^{4+} reference and UO_2^{2+} as U^{6+}. The edge energies of uranium glasses are almost indistinguishable from that of the UO_2 reference while the main edge of UO_2^{2+} is shifted ~2 eV to higher energy indicating that uranium valence in these iron phosphate glasses is 4+.

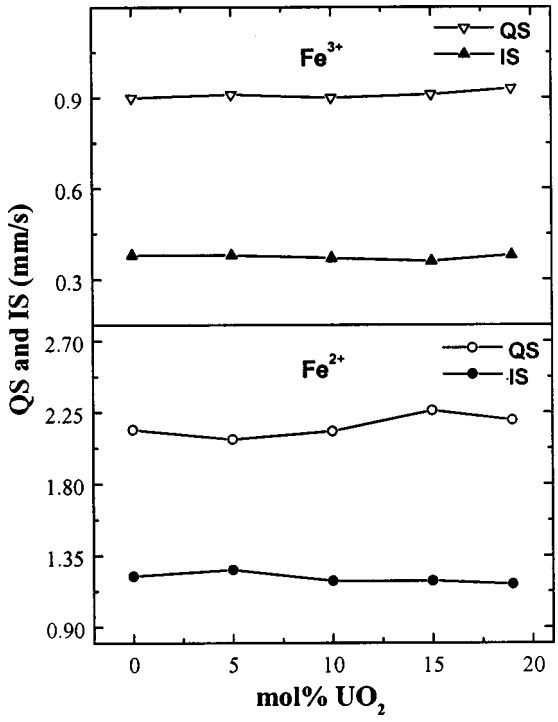

FIG. 8. The quadrupole splittings (QS) and isomer shifts (IS) obtained from room temperature Mössbauer spectra for Fe^{2+} and Fe^{3+} ions in selected iron phosphate glasses. The estimated error in these parameters is less than ±0.05.

increases slightly when only iron is replaced by uranium, glasses F and G. However, glass H, 15 mol% UO_2 is substituted for Fe_2O_3, does not follow this trend.

The U–O coordination numbers obtained from $T^N(r)$ and $T^X(r)$ are approximately four and seven, respectively (see Tables III and IV). The reason for this disparity may be that U–O partial pair correlations in $T^N(r)$ are not well resolved. Uranium ions (U^{4+}) in uranium phosphate compounds and in UO_2[23] have eight-fold coordination with a mean U–O distance of ~2.4 Å. The U–O coordination number of ~7 measured from x-ray scattering in the present study implies that uranium valence in these glasses is close to four, which agree with the XANES results. Uranium ions found in ground water solutions generally have the hexavalent oxidation state as the divalent UO_2^{2+} which is more mobile than the U^{4+} due to the low solubility of uranous phases.[23] If there were U^{6+} ions in the glass, one would expect a lower chemical durability would be expected to compared to the base glass. On the contrary, the dissolution rates, measured in distilled water at 90 °C for 16 days, of $\sim 10^{-9}$ g/cm^2 min for uranium containing iron phosphate glasses, are comparable to that measured for the base glass.[28] Combining this with the fact that the UL_{III}-edge XANES spectra do not show any change in uranium oxidation state, it is highly probable that the peak observed at 1.77 Å in the difference spectrum, $\Delta T(r)$, given in Fig. 6 is due to an artifact such as Fourier termination ripple rather than to a U–O peak. A detailed XANES and EXAFS study on these waste-loaded iron phosphate glasses will be published elsewhere.

The observation that the structural features of uranium containing glasses are similar to those of the base glass is consistent with recent XPS, Raman, and Mössbauer spectroscopic studies of these glasses. As shown in Fig. 8, Mössbauer hyperfine parameters, isomer shift, and quadrupole splitting, do not change appreciably with the uranium content. This indicates that iron environment in glass is not affected by the addition of uranium to a degree detectable by Mössbauer spectroscopy. The second uranium related peak

TABLE V. The structural parameters of the base glass obtained from x-ray and neutron difference spectrum $\Delta T(r)$ (Fig. 4) are compared to the parameters obtained from EXAFS. These parameters are also compared with the structure of crystalline $Fe_3(P_2O_7)_2$ obtained from neutron diffraction (ND).

	$Fe_3(P_2O_7)_2$ polycrystal from ND		Base glass from present study		Base glass from EXAFS	
(ij)	C_{ij}	R_{ij}	C_{ij}	R_{ij}	C_{ij}	R_{ij}
P–O_s	3	1.452	4.1	1.53	···	···
P–O_l	1	1.622	···	···	···	···
Fe–O_s	2.66	1.908	5.5	1.92	3.4	1.90
Fe–O_m	2.00	2.197	1.5	2.29	0.8	2.11
Fe–O_l	1.00	2.404	···	···	0.6	2.35
Fe–P_s	2.66	3.227	4.52	3.25	3	3.18
Fe–P_l	3.33	3.490	···	···	3	3.41

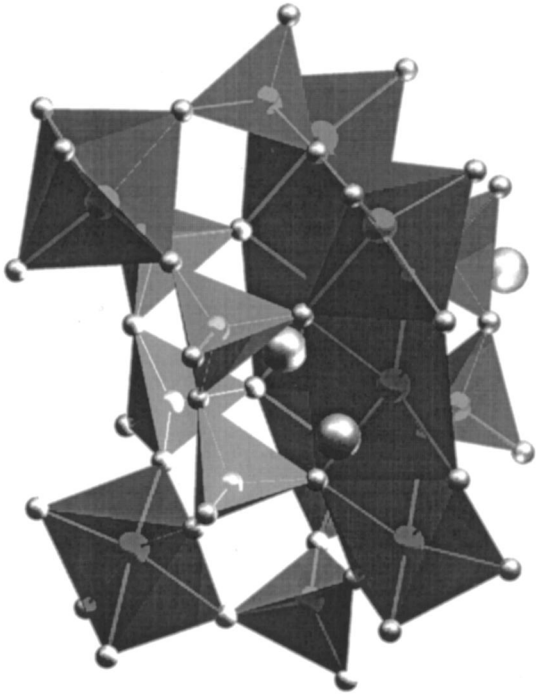

FIG. 9. A three-dimensional illustration of a uranium ion (represented by the larger sphere) placed in the position of a void in the crystal structure of $Fe_3(P_2O_7)_2$. The Fe^{2+} ions in trigonal prism coordination are sandwiched between two Fe^{3+} ions in octahedral coordination which are connected via $(P_2O_7)^{4-}$ groups throughout the network.

in x-ray $T(r)$ is observed at around 3.7 Å (Fig. 3) which indicates that uranium ions are situated far from the Fe–P network in the glass. This may be the reason for the immunity of the Mössbauer hyperfine parameters to the addition of uranium. Both quadrupole splitting and isomer shift are sensitive to the changes in the iron environment. In addition, XPS and Raman spectra of glasses F through H have shown that P–O network features are equally insensitive to the addition of uranium.[29] This insensitivity of the Fe–P–O network to the addition of a nuclear waste component such as uranium may be the reason for the apparent immunity of the chemical durability to the additional waste components.[29]

An in depth analysis of the crystalline structure of $Fe_3(P_2O_7)_2$ helps in explaining some of the observed structural features in these iron phosphate glasses. The average oxygen packing, determined by the average volume per oxygen atom, in $Fe_3(P_2O_7)_2$ is lower than that in most $M_2P_2O_7$ compounds, where M stands for a first raw transition metal.[22] The volume per oxygen atom for $Fe_3(P_2O_7)_2$ and $M_2P_2O_7$ are 19.9 and 17 $Å^3$, respectively. This difference in oxygen packing is due to the voids on each side of $(Fe_3O_{12})^{16-}$ clusters present in the $Fe_3(P_2O_7)_2$ crystal structure. The positions of these voids were determined by looking at the polyhedra around each atom. The suitability of the voids for different waste components were then checked by placing the waste component in the position of a void and calculating near-neighbor distances and volumes of the resulting polyhedra.[30] These voids are found to be large enough to easily host a U^{4+} ion. Figure 9 schematically illustrates an uranium ion placed in one of these voids in the structure of crystalline $Fe_3(P_2O_7)_2$. The density of the base glass and its crystalline counterpart are similar, ~3.1 g/cm^3, which suggest that similar voids may also exist in the glass structure which would explain why Fe–O–P network in glasses containing waste components is similar to that in the base glass. As the glass is quenched from the melt, the Fe–O–P network may form with voids that can be occupied by waste ions such as U^{4+}.

V. CONCLUSION

The structure of iron phosphate glasses containing uranium has been studied by neutron and x-ray diffraction. More detailed structural information can be obtained from the real space correlation functions when the two techniques are used to complement each other. The structural parameters suggest that the basic structural features such as coordination numbers and O–O, P–O distances in uranium containing glasses are the same as those in the base glass. However, a slight change in the Fe–O distances occurs with the addition of uranium. The results obtained in the present study are consistent with the previously obtained XPS and Raman spectroscopic results. The observed structural parameters support a structural model in which the waste elements occupy voids already present in the Fe–O–P network in glass without appreciably altering the basic structure of the parent glass.

ACKNOWLEDGMENTS

This work was supported by the U.S. Department of Energy through the Environmental Management Science Program of the DOE (Contract No. 96ER45618, University of Missouri-Rolla) and the Division of Materials Science, Office of Basic Energy Sciences (Contract W-31-109-EGN-38, Argonne National Laboratory). The author acknowledges with thanks the facility staff of IPNS and APS for their assistance during his stay at ANL where the experiments and data analysis were conducted.

[1] B. C. Sales and L. A. Boatner, in *Radioactive Waste Forms for the Future*, edited by W. Lutze and R. C. Ewing (North-Holland, Amsterdam, 1988), p. 193.
[2] B. C. Sales and L. A. Boatner, Science **226**, 45 (1984).
[3] B. C. Sales, M. M. Abraham, J. B. Bates, and L. A. Boatner, J. Non-Cryst. Solids **71**, 103 (1985).
[4] B. C. Sales, R. S. Ramsey, J. B. Bates, and L. A. Boatner, J. Non-Cryst. Solids **87**, 137 (1986).
[5] L. A. Chick, L. R. Bunnel, D. M. Strachen, H. E. Kissinger, and F. N. Hodges, PNL-5878, Hanford WA, 1986.
[6] G. K. Marasinghe *et al.*, J. Non-Cryst. Solids **222**, 144 (1997).
[7] D. E. Day, Z. Wu, C. S. Ray, and P. Hrma, J. Non-Cryst. Solids **241**, 1 (1998).
[8] X. Yu, D. E. Day, G. J. Long, and R. K. Brow, J. Non-Cryst. Solids **215**, 21 (1997).
[9] C. H. Booth *et al.*, J. Mater. Res. **14**, 2628 (1999).
[10] G. K. Marasinghe, M. Karabulut, C. S. Ray, D. E. Day, C. H. Booth, P. G. Allen, and D. K. Shuh, Ceram. Trans. **87**, 261 (1998).
[11] B. C. Bunker, G. W. Arnold, and J. A. Wilder, J. Non-Cryst. Solids **64**, 291 (1984).
[12] D. L. Price, A. J. G. Ellison, M.-L. Saboungi, R. Z. Hu, T. Egami, and W. S. Howels, Phys. Rev. B **55**, 11249 (1997).
[13] P. Armand, M. Beno, A. J. G. Ellison, G. S. Knapp, D. L. Price, and M.-L. Saboungi, Europhys. Lett. **29**, 549 (1995).
[14] Y. Waseda, *The Structure of Non-crystalline Materials* (McGraw-Hill, New York, 1980).

[15] U. Hoppe, G. Walter, D. Stachel, and A. C. Hannon, Z. Naturforsch. A **51**, 179 (1996).
[16] H. F. Poulsen, J. Neuefeind, H. B. Neumann, J. R. Schneider, and M. D. Zeidler, J. Non-Cryst. Solids **188**, 63 (1995).
[17] C. S. Ray, X. Fang, M. Karabulut, G. K. Marasinghe, and D. E. Day, J. Non-Cryst. Solids **249**, 1 (1999).
[18] A. J. G. Ellison, R. K. Crawford, D. G. Montague, K. J. Volin, and D. L. Price, J. Neutron Res. **1**, 61 (1993).
[19] A. C. Wright and A. J. Leadbetter, Phys. Chem. Glasses **17**, 122 (1976).
[20] D. L. Price, M.-L. Saboungi, Y. S. Badyal, J. Wang, S. C. Moss, and R. L. Leheny, Phys. Rev. B **57**, 10496 (1998).
[21] S. Susman, K. J. Volin, D. G. Montague, and D. L. Price, J. Non-Cryst. Solids **125**, 168 (1990).
[22] M. Ijjaali, G. Verturini, R. Geradin, B. Malaman, and C. Gleitzer, Eur. J. Solid State Inorg. Chem. **28**, 983 (1991).
[23] N. C. Sturchhio, M. R. Antorio, L. Soderholm, S. R. Sutton, and J. C. Brannon, Science **281**, 971 (1998).
[24] K. Suzuki and M. Uneo, J. Phys. (Paris) **46**, c8-261 (1985).
[25] U. Hoppe, G. Walter, D. Stachel, and A. C. Hannon, Z. Naturforsch. A **50**, 684 (1996).
[26] S. R. Elliot, J. Non-Cryst. Solids **182**, 40 (1995).
[27] P. H. Gaskell and D. J. Wallis, Phys. Rev. Lett. **76**, 66 (1996).
[28] M. Karabulut, G. K. Marasinghe, C. S. Ray, D. E. Day, O. Ozturk, and G. D. Waddill, J. Non-Cryst. Solids **249**, 106 (1999).
[29] G. K. Marasinghe *et al.*, Ceram. Trans. **93**, 195 (1999).
[30] E. Koch and W. Fischer, Z. Kristallogr. **211**, 251 (1996).